

Effect of Screw Rotation Speed on the Properties of Polystyrene/Organoclay Nanocomposites Prepared by a Twin-Screw Extruder

Shuichi Tanoue,¹ Aniwat Hasook,¹ Takumi Itoh,¹ Masaharu Yanou,¹ Yoshiyuki Iemoto,¹ Tsunemune Unryu²

¹Department of Materials Science and Engineering, University of Fukui, 3-9-1 Bunkyo, Fukui 910-8507, Japan

²Industrial Technology Center of Fukui Prefecture, 61-10 Kawaiwashizuka-cho, Fukui-shi, Fukui 910-0102, Japan

Received 22 June 2005; accepted 15 December 2005

DOI 10.1002/app.24004

Published online in Wiley InterScience (www.interscience.wiley.com).

ABSTRACT: We discuss the effect of screw rotation speed on the mechanical and rheological properties and clay dispersion state of polystyrene (PS)/organoclay (clay) nanocomposites prepared by melt compounding with a counter-rotating-type twin-screw extruder. Poly(styrene-co-vinylloxazolin) (OPS) was used as an additional material. The Young's modulus of the PS/OPS/clay nanocomposites showed the maximum value at a screw rotation speed of 70 rpm in this study. This implied the existence of an optimized screw rotation speed for the melt compounding of the polymer/clay nanocomposites. For PS/clay systems without the addition of OPS, the peak intensity from clay increased and the distance between clay platelets in the nanocomposites decreased with the screw rotation speed. On the other hand, inverse results were obtained for PS/OPS/clay systems.

According to the transmission electron microscopy photographs, the PS/OPS/clay nanocomposite at 70 and 100 rpm had fully exfoliated clay platelets. The dynamic rheological properties of the PS/clay nanocomposites were almost the same as those of neat PS. On the other hand, the storage and loss moduli of the PS/OPS/clay nanocomposites at the same frequency were larger than those of the PS/clay system. On the whole, the bonding between clay platelets and PS was important for increasing the viscosity and elasticity in the melts of the PS/clay system. © 2006 Wiley Periodicals, Inc. *J Appl Polym Sci* 101: 1165–1173, 2006

Key words: melt; nanocomposites; organoclay; polystyrene; processing

INTRODUCTION

Polymer/clay nanocomposites are materials that comprise a dispersion of nanometer-size clay platelets in a polymer matrix. A significant improvement in several properties (e.g., Young's modulus, thermal stability, fire retardancy, gas barrier) can be accomplished by the dispersion of a small amount of nanometer-size clay platelets in the polymer matrix.¹ For example, the incorporation of 4.2 wt % of exfoliated montmorillonite (MMT) into polyamide 6 (PA-6) increases the Young's modulus by a factor of 2.1.² There are two representative methods for the preparation of polymer/clay nanocomposites: (1) a reaction method such as polymerization or stirring in a solution and (2) a melt compounding method in which a polymer and clay are mixed at a higher melting temperature. Melt compounding is useful in industry because (1) it is rapid, less than about 10 min, and (2) it uses existing mixing equipment, such as a twin-screw extruder.

A typical polymer/clay nanocomposite system is PA-6/clay. This system is comparatively easy to prepare a polymer/clay nanocomposite with fully exfoliated clay platelets by melt compounding. Therefore, several researchers have studied the melt compounding process of polymer/clay nanocomposites with PA-6/clay systems. Dennis et al.³ studied the melt compounding process of PA-6/organoclay nanocomposites with various twin-screw extruders and mixers. They concluded that clay dispersion states in the polymer matrix were dependent on residence time and were independent of screw configuration. Davis et al.⁴ studied the process conditions of poly(ethylene terephthalate)/MMT nanocomposites by melt compounding with a batch kneader. Alternative mixing conditions, a longer residence time, and higher screw speeds resulted in lower quality nanocomposites. Shah and Paul⁵ investigated the utility of masterbatch process for the preparation of polymer/clay nanocomposites by melt compounding with PA-6 organoclay as a model system. Fornes et al.⁶ investigated the effect of the molecular weight of nylon 6 on the properties of nylon 6/organoclay nanocomposites by melt compounding. Hasegawa et al.⁷ developed a preparation method with a water slurry of Na-MMT for PA-6/

Correspondence to: S. Tanoue (tanoue@matse.fukui-u.ac.jp).

MMT nanocomposites by melt compounding. Other studies of melt compounding process for the preparation of polymer/clay nanocomposites have been carried out by other researchers with other polymers, such as polycarbonate,^{8,9} polypropylene (PP),¹⁰ ethylene–vinyl alcohol,^{11,12} epoxy,¹³ and green plastics such as Poly(L-lactic acid) (PLLA).¹⁴

Polystyrene (PS) is one polymer with which it is difficult to obtain the fully exfoliated clay platelets in its polymer/clay nanocomposites. Because PS is a nonpolar polymer, the bonding forces between the surface of the clay platelets and the polymer matrix become weak. Tanoue and coworkers^{15–17} studied the process conditions for the preparation of PS/organoclay nanocomposites with a twin-screw extruder. Wang et al.¹⁸ investigated the properties of PS/organoclay nanocomposites with three kinds of organoclay by melt compounding. However, PS/clay nanocomposites with fully exfoliated clay platelets could not be obtained by direct melt compounding with PS and organoclay only. Therefore, some additional technique is necessary to prepare PS/clay nanocomposite with exfoliated clay platelets by melt compounding. One of these solutions is the use of a new organoclay with good performance for the preparation of PS/clay nanocomposites. For example, Hoffmann et al.¹⁹ used amine-terminated PS with a number-average molecular weight of 5800 g/mol as an organic modifier of the clay. They obtained a PS/clay nanocomposite with fully exfoliated clay platelets by melt compounding. Other solutions were used as additional materials, such as a plasticizer or compatibilizer with good performance, for the preparation of PS/clay nanocomposites by melt compounding. This is a comparatively easy application. In case of PP, maleic anhydride grafted PP is useful for the preparation of PP/clay nanocomposites with fully exfoliated clay platelets in the polymer matrix by melt compounding.²⁰ We can easily guess that it is necessary to use some additional materials, such as maleic anhydride grafted PP, for PS. Hasegawa et al.²¹ used poly(styrene-*co*-vinylloxazolin) (OPS) as an additional material. They obtained PS/clay nanocomposites with fully exfoliated clay platelets by melt compounding with a twin-screw extruder. Yoon et al.²² investigated the effect of polar comonomers in PS chains on the melt intercalation with a commercialized organoclay. They focused acrylonitrile and methylvinylloxazoline comonomers. Their obtained nanocomposites did not show an exfoliated structure, although the structure of the copolymer hybrids was very stable under long mixing times. As mentioned previously, OPS seems to be useful for the preparation of PS/clay nanocomposite with exfoliated clay platelets by melt compounding. The next target of the study of PS/clay nanocomposites with an additional materials, such as OPS, by melt compounding will be the process conditions, for example, barrel

temperature, screw rotation speed, compounding ratio, and feed rate.

The aim of this study was to provide guidelines for the melt compounding of PS-based nanocomposites with a commercialized organoclay. We selected a range of screw rotation speeds from several functions of melt compounding with a twin-screw extruder. In this article, we present the effects of screw rotation speed on the mechanical and rheological properties and the dispersion state of the clay platelets of PS/organoclay nanocomposites with OPS by melt compounding.

EXPERIMENTAL

Materials

The commercialized PS used in this study was kindly supplied by PS Japan Co., Ltd. (Tokyo, Japan). This PS was a commercial product of PS Japan with the grade name HF77. The selected organoclay (i.e., clay) was S-Ben NZ, which was kindly supplied by Hojun, Co., Ltd. (Annaka, Japan). This organoclay was a bentonite [cation exchange capacity (CEC) = 0.93 mequiv/g] intercalated by dimethyl benzyl stearyl ammonium ions. It is generally difficult to produce fully exfoliated PS/organoclay nanocomposites because PS is a nonpolar polymer. Therefore, it may be necessary to use some compatibilizer when PS/organoclay nanocomposites are prepared by melt compounding. OPS, which was a commercial product of Nihon Shokubai, Co., Ltd. (Osaka, Japan), with the grade name EP-OCROS RPS1005, was used as the compatibilizer in this study because fully exfoliated PS/organoclay nanocomposites could be produced by melt compounding and with OPS as the compatibilizer.²² About 3–5 wt % oxazolin units was included in OPS. Other properties of the materials used are listed in Table I.

Melt compounding of PS with organoclay

Table II shows the composition of the nanocomposites prepared in this study. The organoclay contents of PS/clay and PS/OPS/clay were set up at 5 wt %. PS, OPS, and clay were mixed in a counter-rotating twin-screw extruder manufactured by Musashino Kikai, Co., Ltd. (Tokyo, Japan). It had a screw diameter of 25 mm and a screw length/diameter ratio of 28. Figure 1 shows the schematic of the apparatus used for the preparation of the nanocomposites. PS, OPS, and clay were dried in vacuo at 50°C for at least 24 h before compounding. Clay was added to the molten polymer with a side feeder. OPS was added to the pellet polymer by a side feeder from the position shown in Figure 1. Compounding was carried out at a uniform barrel temperature of 180°C and a feed rate of 5 kg/h

TABLE I
Material Characteristics

Material (Code)	Supplier	Specification
Polystyrene HF-77 (PS)	PS Japan	$M_w = 216,500$ MFR = 7.5 g/10 min
Poly(styrene-co-vinylloxazoline) EPOCROS RPS1005 (OPS)	Nihon Shokubai	$M_w = 170,000$ –180,000 3–5 wt % oxazolin unit was included.
Organoclay S-Ben NZ (clay)	Hojun	Bentonite intercalated with dimethyl benzyl stearyl ammonium ion intercalated between clay platelets; CEC of bentonite = 0.93 mequiv/g; organic content = 37.9 wt %; interlayer spacing: $d_{001} = 4.01$ nm.

M_w = weight-average molecular weight; MFR = melt flow rate.

for each sample. We selected four screw rotation speeds, 20, 40, 70, and 100 rpm, for each PS/organoclay nanocomposite.

Tensile testing

The specimens for tensile testing (JIS K7162, type 1BA) were prepared by a handy injection-molding machine at a barrel temperature of 200°C. The samples were dried *in vacuo* at 50°C for at least 24 h before molding. After molding, the molded specimens were kept at room temperature for at least 48 h because of the relaxation of elasticity in the specimens. Tensile tests were carried out at room temperature according to JIS K7162 with a Shimadzu Autograph AGS-J (Kyoto, Japan). Young's modulus was measured with an extensometer. The crosshead speed was set up at 1 mm/min.

X-ray diffraction (XRD) and transmission electron microscopy (TEM)

The dispersed state of the clay layers in the matrix polymer was evaluated with XRD and TEM. XRD spectra were obtained with a Rigaku SWXD-FK X-ray diffractometer (Cu K α radiation with $\lambda = 1.5406$ Å; Tokyo, Japan). XRD measurements were carried out in a 2θ scan range of 1–10° at a scanning rate of 0.5°/min and at room temperature. The specimens of the nanocomposites for XRD measurements were obtained in sheet form with a heat press at temperature of 180°C and a compression pressure of 19.6 MPa.

For the preparation of the samples for TEM photographs, the plate-type specimens with thicknesses of 5

mm were prepared by a heat press under a press temperature of 180°C, a molding pressure of 4.9 MPa, a preheating time of 5 min, a heat press time of 5 min, a cooling press temperature of 30°C, and a cooling press time of 3 min. The samples for TEM analysis were all microtomed at room temperature with a diamond knife with a microtome (Leichert-Nissei Ultracut N, FC 4D, Tokyo, Japan). The thickness of the sections was 70 nm. TEM photographs were taken with a Hitachi Seisakusho Co. H-8000 instrument (Tokyo, Japan) at an accelerating voltage of 200 kV.

Rheological measurement

For rheological characterization, various nanocomposites were measured with a rheometer (ARES, Rheometrics Scientific FE) with parallel-plate geometry. A frequency sweep test was carried out at 180 and 220°C with 5% strain, which was within the linear viscoelastic region. All measurements were conducted under a dry air environment. The experimental error of each rheological datum from some degradation of PS at a high temperature was about 10%.

RESULTS AND DISCUSSION

Tensile testing

Figure 2 shows the tensile testing results of the composites at various screw rotation speeds. The Young's modulus of neat PS was almost independent of the

TABLE II
Compositions of the Nanocomposites

Sample	PS (wt %)	OPS (wt %)	Clay (wt %)
PS/OPS/clay	95	0	5
PS/clay	50	45	5
PS	100	0	0

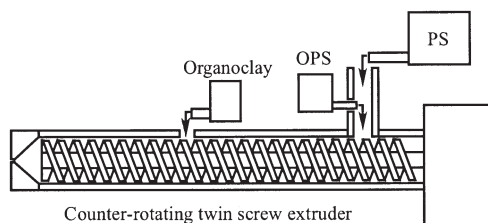


Figure 1 Illustration of apparatus used in melt compounding.

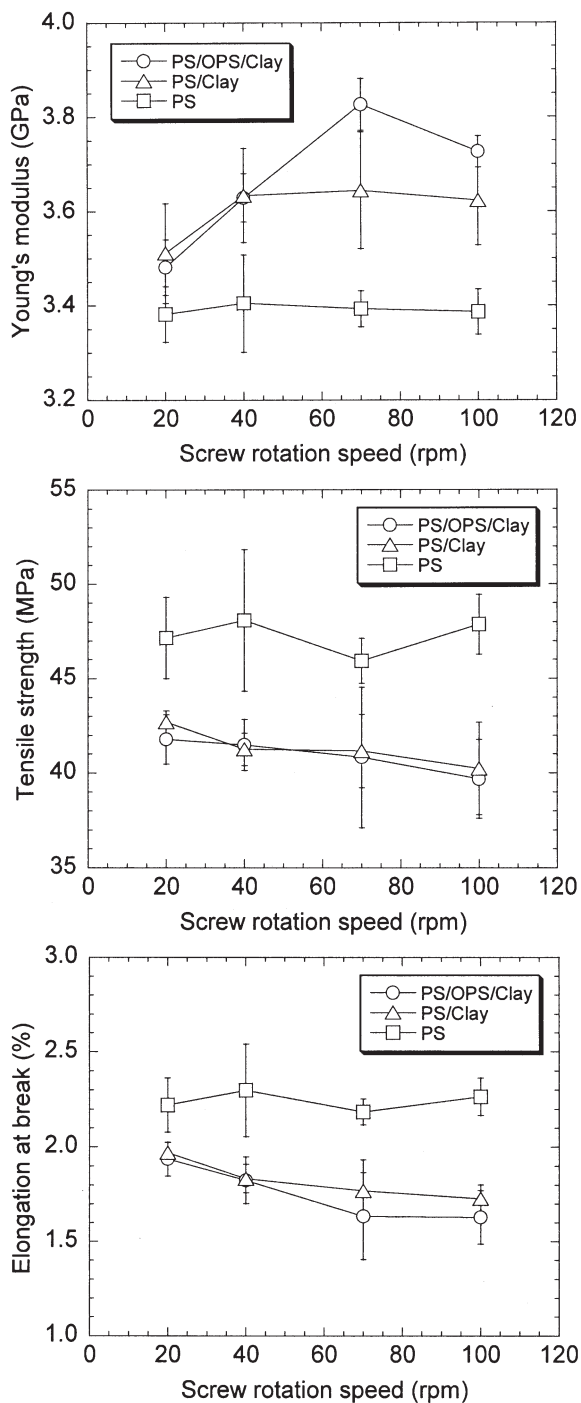


Figure 2 Tensile testing results as a function of screw rotation speed for various PS-based composites prepared by a counterrotating twin-screw extruder. The organoclay content of the PS-based organoclay composites PS/clay and PS/OPS/clay was 5 wt %.

screw rotation speed. The Young's modulus of the PS/clay nanocomposites increased with screw rotation speed at low speeds (20–40 rpm) and became almost constant with increasing screw rotation speed; it was about 7% larger than that of neat PS at screw rotation speeds greater than 40 rpm. The Young's

modulus of the PS/OPS/clay nanocomposite at screw rotation speeds of 20–40 rpm was almost the same as that of PS/clay. This Young's modulus showed a maximum value at a screw rotation speed of 70 rpm and was about 20% larger than that of neat PS at a screw rotation speed of 70 rpm. This result implied the existence of an optimum screw rotation speed for the melt compounding of polymer/clay nanocomposites with a twin-screw extruder.

The tensile strength of each composite was almost independent of the screw rotation speed. The tensile strength of the PS/clay nanocomposites was about 10% smaller than that of neat PS and was almost the same as that of PS/OPS/clay. Similar patterns were seen for elongation at break.

Also, the tensile strength and the elongation at break of the PS/clay nanocomposites were independent of the addition of OPS to the PS/clay nanocomposite system by melt compounding, although this addition influenced the Young's modulus at high screw rotation speeds.

XRD results

Figure 3 shows the XRD results of PS/clay and PS/OPS/clay nanocomposites prepared by a twin-screw extruder at each screw rotation speed. The XRD results of neat organoclay and PS are also shown in the same figures. There were two peaks in each XRD result for the PS/clay nanocomposites. Because the intensity of the first peak was larger than that of the second peak, it was possible to judge that the first peak was from d_{001} and that the second peak was from d_{002} . Therefore, d_{001} estimated by Bragg's formula was the d -spacing between clay platelets. The intensity of the first peak for the PS/clay nanocomposites increased with screw rotation speed, although the first peak intensity decreased with screw rotation speed for the PS/OPS/clay nanocomposites. The first and second peaks disappeared at a screw rotation speed of 100 rpm. This composite may have been exfoliated.

As mentioned previously, the d -spacing between clay platelets could be estimated by Bragg's formula with 2θ of the first peak. Figure 4 shows the d -spacing as a function of screw rotation speed. The d -spacing of the neat organoclay estimated from the XRD results shown in Figure 3 is also shown in Figure 4. It was difficult to estimate the d -spacing for the PS/OPS/clay at screw rotation speed of 100 rpm because there was a very small peak from d_{001} in this XRD result. Therefore, this value may not be accurate. The d -spacing of PS/OPS/clay was larger than that of PS/clay. Because the bonding force between the PS matrix and the clay in the PS/OPS/clay system was larger than that in the PS/clay system, the clay in the PS/OPS/clay system was sensitive to flow in the twin-screw extruder. The d -spacings of PS/OPS/clay and PS/clay increased

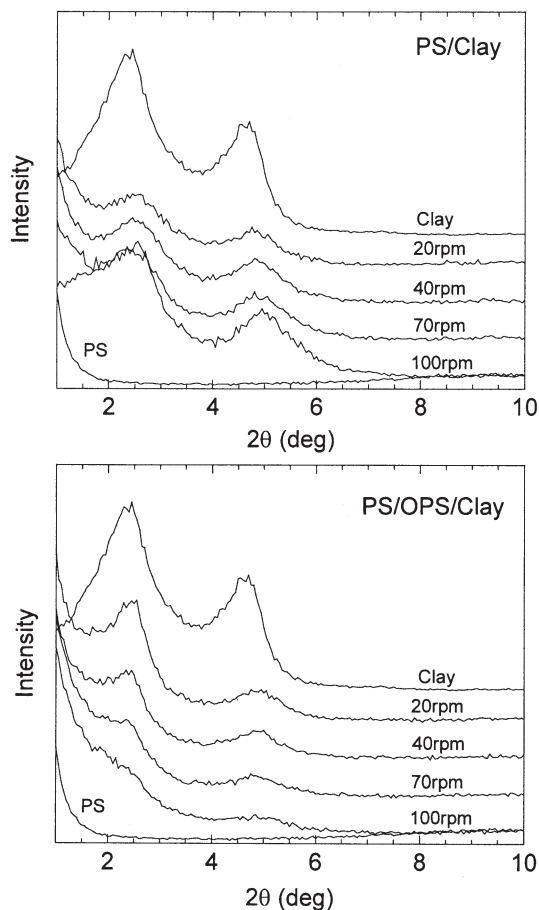


Figure 3 XRD results of PS-based organoclay nanocomposites at various screw rotation speeds. The organoclay content of the PS-based organoclay composites PS/clay and PS/OPS/clay was 5 wt %. The XRD results of neat PS and the neat organoclay are shown in each section.

with screw rotation speed, except for that of PS/OPS/clay at a screw rotation speed of 100 rpm. This result implies that the degree of shear and elongation had an effect on the d -spacing of the clay in the PS/clay and PS/OPS/clay nanocomposites. However, the d -spacings of all PS/clay cases and PS/OPS/clay nanocomposites prepared at a low screw rotation speed (20 rpm) were smaller than that of the neat organoclay. This tendency was not seen in past studies on PS/organoclay nanocomposites. One possibility is that extra intercalant between clay platelets may have been extruded by the high temperature during melt compounding. When organoclay was added to the molten neat PS, extra intercalant between the clay platelets may have been extruded at once. After that, the d -spacing of clay would have expanded by shear and elongation during melt compounding by the twin-screw extruder.

TEM photographs

It was important to check the state of clay dispersion in the PS/clay nanocomposites with TEM photo-

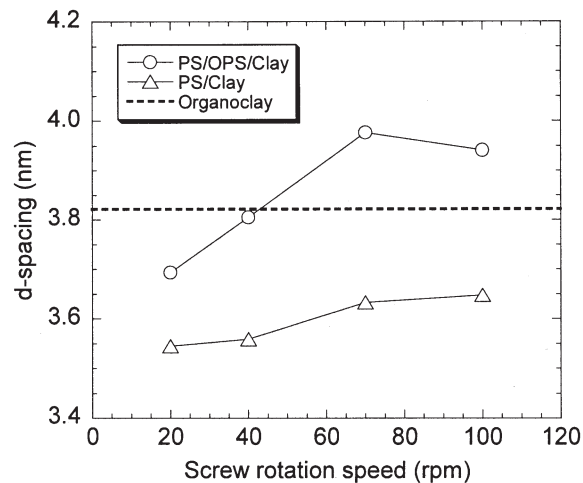


Figure 4 d -spacings of the PS/organoclay nanocomposites as a function of the screw rotation speed. The organoclay content of the PS-based organoclay composites PS/clay and PS/OPS/clay was 5 wt %.

graphs. We checked the clay dispersion state of our prepared mixtures by taking TEM photographs. Figure 5 shows the TEM photographs of the PS/clay nanocomposites at various screw rotation speeds. We observed large clay lumps with many clay stacks at 20 rpm. Although this size seemed to decrease with screw rotation speed, we observed several clay lumps with clay stacks at 100 rpm. The clay was not completely exfoliated in the PS/clay system prepared using the twin-screw extruder. It seemed difficult to prepare the exfoliated PS/organoclay nanocomposite with our counterrotating twin-screw extruder even when the screw rotation speed was set up at a high value of 100 rpm.

Figure 6 shows the TEM photos of the PS/OPS/clay nanocomposites at various screw rotation speeds. At low screw rotation speeds (20 and 40 rpm), there were some clay lumps, including clay platelets, in the mixtures. However, some clay seemed to be exfoliated at screw rotation speeds of 70 and 100 rpm. These results corresponded with the XRD diffraction results. Even when OPS was used as a compatibilizer for the preparation of the PS/clay nanocomposites by melt compounding with the twin-screw extruder, we did not obtain exfoliated PS/clay nanocomposites at a low screw rotation speed (20 rpm). Our obtained results imply the existence of an optimum screw rotation speed and the necessity of physical force from shear and elongation flow for the preparation of exfoliated nanocomposite by melt compounding.

Rheological testing results

The rheological properties of polymer/clay nanocomposites are important in the consideration of polymer

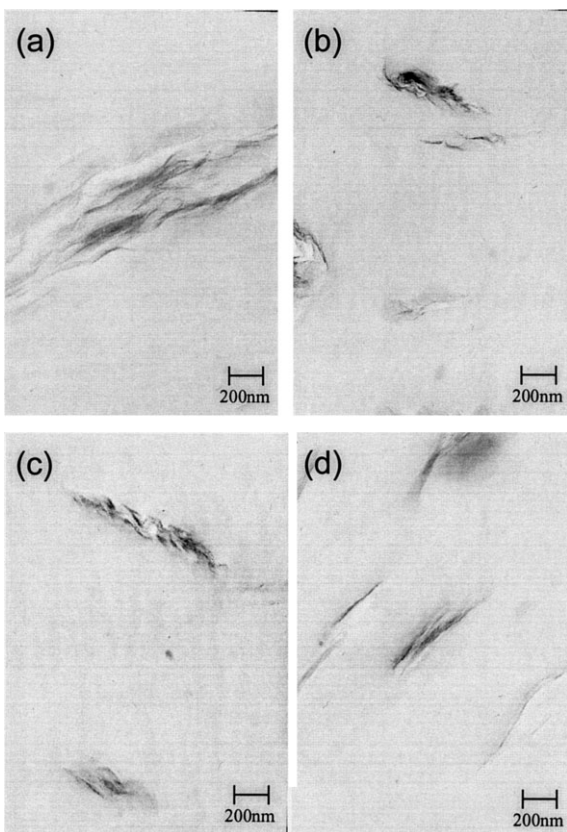


Figure 5 TEM photos of PS/clay nanocomposites prepared by a twin-screw extruder at various screw rotation speeds (barrel temperature = 180°C, organoclay content = 5 wt %). Screw rotation speeds = (a) 20, (b) 40, (c) 70, and (d) 100 rpm.

processing using polymer/clay nanocomposites processing because polymer processing is one of the fluid operations of polymer melts. We measured the rheological properties of our prepared nanocomposites and considered the relationship between the rheological properties and structure and process conditions. Figures 7 and 8 show the storage modulus (G') and loss modulus (G'') of the PS/organoclay nanocomposites at a temperature of 180°C. Figure 7 shows a screw rotation speed of 20 rpm, and Figure 8 is at 70 rpm. In these figures, a_T is the horizontal shift factor, and b_T is the vertical shift factor defined by the following equation:

$$b_T = \frac{\rho T}{\rho_0 T_0} \quad (1)$$

where ρ is the density at temperature T and ρ_0 is the density at the reference temperature T_0 . G' and G'' of the PS/clay composites were almost the same as those of PS except for G' of the PS/clay composite prepared at a screw rotation speed of 70 rpm at low frequency. G' and G'' of the PS/OPS/clay composite were larger than those of the other composites (PS and PS/clay)

on the whole. In practice, G' of the PS/OPS/clay composite prepared at 70 rpm showed a higher value than those of the other composites at low frequency ($< \omega a_T = 0.1$ rad/s, ω is the frequency). This implied that these tendencies may have been due to the strong bonding force between the clay plate and PS matrix and intercalation or exfoliation of clay platelets by mixing with OPS.

The dynamic viscosity (η') and the storage modulus coefficient (ψ') were defined by the following equations:

$$\eta' = G'' / \omega \quad (2)$$

$$\psi' = G' / \omega^2 \quad (3)$$

These values were obtained by the previous equations and with the G' and G'' curves in Figures 7 and 8. Figure 9(a) shows η' as a function of frequency at a screw rotation speed of 70 rpm. η' of PS/clay was almost the same as that of PS on the whole. η' of PS/OPS/clay was larger than that of PS, especially in the low-frequency region. Figure 9(b) shows ψ' as a function of frequency at a screw rotation speed of 70

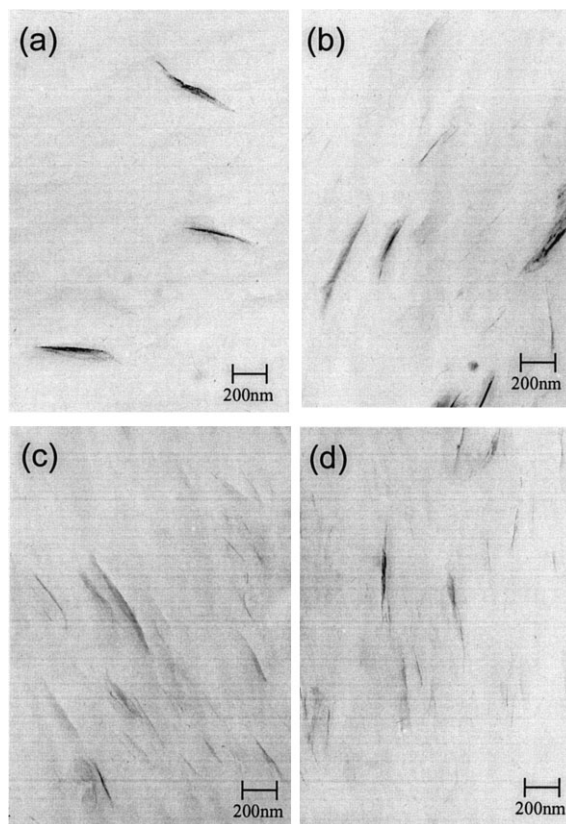


Figure 6 TEM photos of PS/OPS/clay nanocomposites prepared by a twin-screw extruder at various screw rotation speeds (barrel temperature = 180°C, organoclay content = 5 wt %). Screw rotation speeds = (a) 20, (b) 40, (c) 70, and (d) 100 rpm.

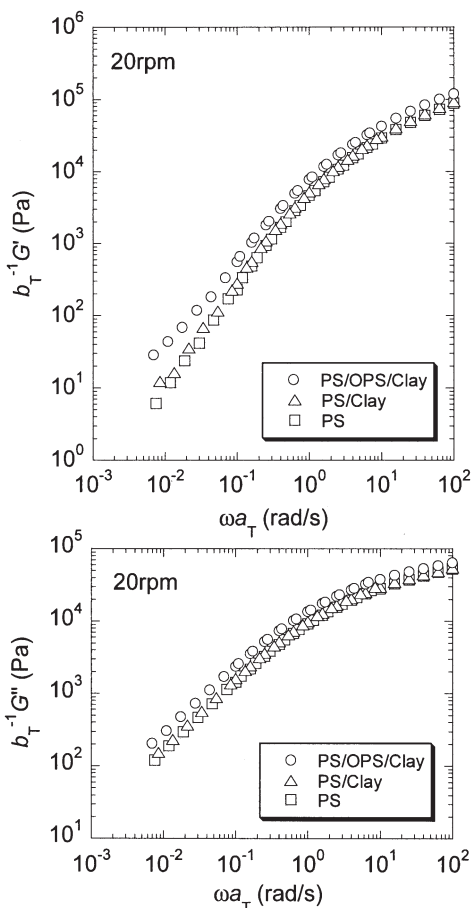


Figure 7 G' and G'' values of PS/organoclay nanocomposites prepared by melt compounding with a twin-screw extruder ($T_0 = 180^\circ\text{C}$, organoclay content = 5 wt %). PS = neat PS, PS/clay = PS-based organoclay nanocomposites; PS/OPS/clay = PS-based and OPS-based organoclay nanocomposites.

rpm. ψ' of PS/OPS/clay was the largest of the three composites. In the low-frequency region, ψ' of PS/clay was larger than that of PS. However, both were almost the same at $\omega a_T > 0.05$ rad/s. These curves could be fitted by the Carreau–Yasuda type equation as follows:

$$\eta' = \eta_0(1 + K_v \omega^{m_1})^{m_2} \quad (4)$$

$$\psi' = \psi_0(1 + K_s \omega^{n_1})^{n_2} \quad (5)$$

where η_0 is the zero-shear viscosity, ψ_0 is the zero-shear storage modulus coefficient, and K_v , K_s , m_1 , m_2 , n_1 , and n_2 are material constants. The viscosity and elasticity of each material at a low shear rate could be cleared by η_0 and ψ_0 obtained by fitting with eqs.(4) and (5). Figure 10(a) shows the η_0 of PS, PS/clay, and PS/OPS/clay as a function of screw rotation speed. η_0 of PS/clay was almost the same as that of PS. η_0 of PS/OPS/clay was larger than that of PS and PS/clay

on the whole. According to the TEM photographs in Figure 6, the clay dispersion state of PS/OPS/clay at a low screw rotation speed (20 rpm) was almost the same as that of PS/clay at the same screw rotation speed (20 rpm). However, η_0 of the PS/OPS/clay at 20 rpm was about 1.7 times larger than that of PS/clay, although the η_0 values of PS/clay and PS were almost the same at various screw rotation speeds. η_0 of PS/OPS/clay at 70 rpm was the maximum value, and η_0 of PS/OPS/clay at 70 rpm was about 1.4 times larger than that at 20 rpm. According to the TEM photographs in Figure 6, PS/OPS/clay at 70 rpm had some exfoliated clay platelets, but PS/OPS/clay at 20 rpm had no exfoliated clay platelets. Therefore, the difference in η_0 of PS/OPS/clay between 20 and 70 rpm caused the clay dispersion states. However, this difference was smaller than that between PS/clay and PS/OPS/clay. In addition, η_0 of PS/clay was almost the same as that of PS at each screw rotation speed. The viscosity of the PS/clay nanocomposite system

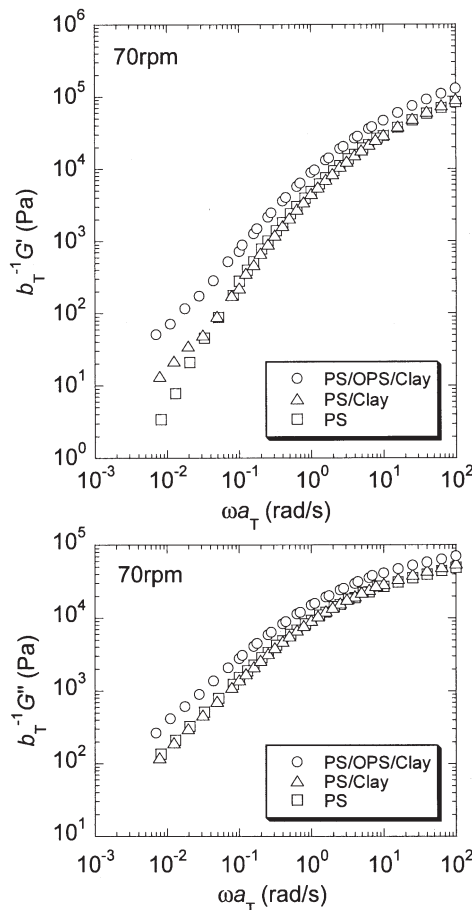


Figure 8 G' and G'' values of PS/organoclay nanocomposites prepared by melt compounding with a twin-screw extruder ($T_0 = 180^\circ\text{C}$, organoclay content = 5 wt %). PS = neat PS, PS/clay = PS-based organoclay nanocomposites; PS/OPS/clay = PS-based and OPS-based organoclay nanocomposites.

depended not on the dispersion state of the clay platelets in the materials but on the bonding between the clay platelets and matrix polymer (PS) by oxazolin units in OPS. Figure 10(b) shows the ψ_0 values of PS, PS/clay, and PS/OPS/clay as a function of screw rotation speed. At the same screw rotation speed, ψ_0 of PS/clay was larger than that of PS, and ψ_0 of PS/OPS/clay was larger than that of PS/clay. For PS/OPS/clay, ψ_0 at 70 rpm was the maximum value. ψ_0 of PS/OPS/clay at 70 rpm was about 15 times larger than that at 20 rpm. This may have been caused by bonding between the clay platelets and PS by oxazolin units in OPS and the clay dispersion state. On the whole, the bonding between clay platelets and PS was important for increasing the viscosity and elasticity for the melts of the PS/clay system. In addition, the clay dispersion state also affected the flow characteristics of the PS/clay melt.

CONCLUSIONS

We discussed the effect of screw rotation speed on mechanical and rheological properties and the disper-

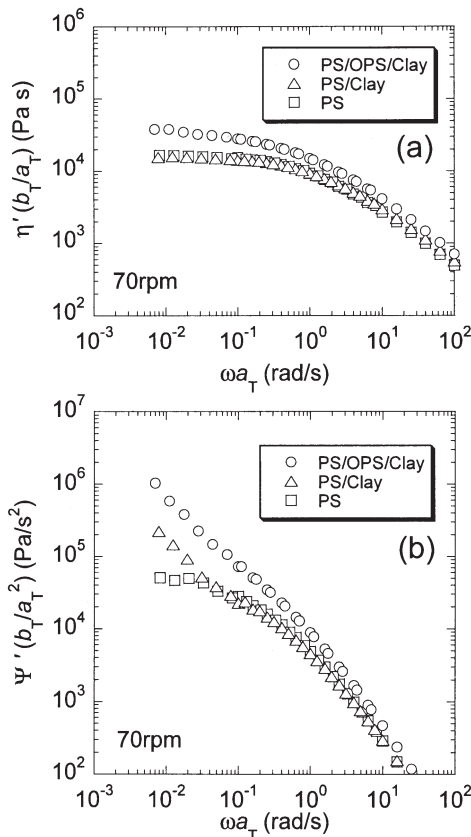


Figure 9 (a) η' and (b) ψ' as a function of frequency for PS/organoclay nanocomposites prepared by melt compounding ($T_0 = 180^\circ\text{C}$, screw rotation speed = 70 rpm, organoclay content = 5 wt %). PS = neat PS, PS/clay = PS-based organoclay nanocomposites; PS/OPS/clay = PS-based and OPS-based organoclay nanocomposites.

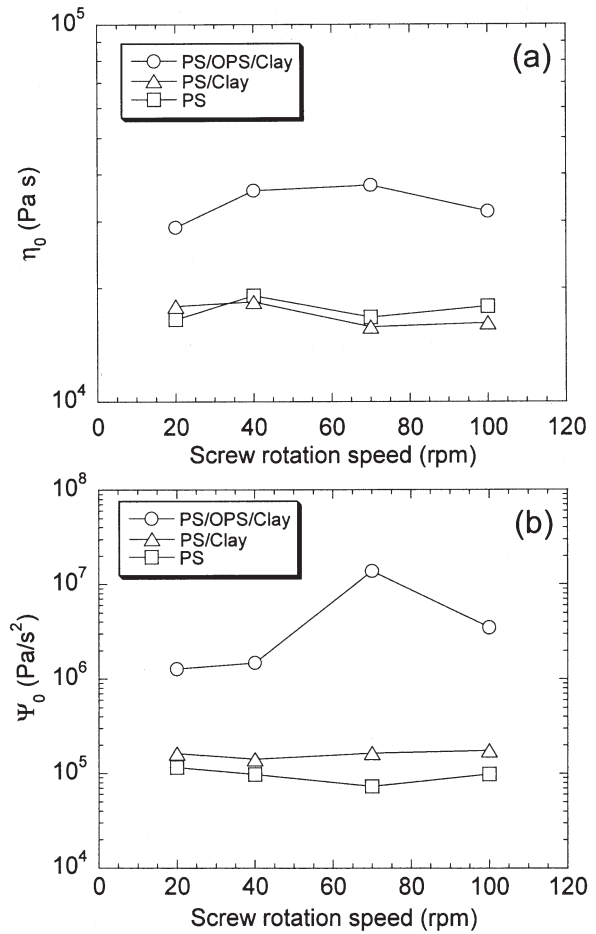


Figure 10 (a) η_0 and (b) ψ_0 as a function of screw rotation speed for PS/organoclay nanocomposites prepared by melt compounding ($T_0 = 180^\circ\text{C}$, organoclay content = 5 wt %). PS = neat PS, PS/clay = PS-based organoclay nanocomposites; PS/OPS/clay = PS-based and OPS-based organoclay nanocomposites.

sion state of clay platelets of PS/organoclay (clay) nanocomposites with OPS by melt compounding with a counter-rotating twin-screw extruder. The following results were obtained.

The Young's modulus of the PS/clay nanocomposites at low screw rotation speeds (20 and 40 rpm in this study) was almost the same as that of PS/OPS/clay. At high screw rotation speeds (70 and 100 rpm in this study), the Young's modulus of the PS/OPS/clay nanocomposite was larger than that of PS/clay, and that of PS/OPS/clay at 70 rpm was the maximum value. These results imply the existence of an optimum screw rotation speed for the melt compounding of the polymer/clay nanocomposite with a twin-screw extruder, at least for the PS/clay system.

The clay dispersion state in the PS/clay nanocomposites depended on the screw rotating speed during melt compounding. For the PS/clay system without OPS, the peak intensity from the clay increased, and the distance between the clay platelets in the PS/clay

nanocomposite decreased with screw rotation speed. On the contrary, for the PS/OPS/clay system, the peak intensity from the clay decreased, and the distance of clay platelets in the PS/OPS/clay nanocomposite increased with screw rotation speed. These clay dispersion states were confirmed by TEM photographs. In this study, the PS/OPS/clay nanocomposite at 70 and 100 rpm had fully exfoliated clay platelets.

The dynamic rheological properties of the PS/clay nanocomposites were almost the same as those of neat PS. On the other hand, G' and G'' of the PS/OPS/clay nanocomposites at the same frequency were larger than those of the PS/clay system. These tendencies could especially be seen for the nanocomposites prepared at a low screw rotation speed (20 rpm in this study), even when the tensile properties and clay dispersion state of the PS/OPS/clay nanocomposites prepared at the low screw rotation speed were almost the same as those of PS/clay prepared at the same screw rotation speed. On the whole, the bonding between the clay platelets and PS was important for increasing the viscosity and elasticity of the melts of the PS/clay system.

In general, the Young's modulus of the polymer/clay nanocomposites with fully exfoliated clay platelets was 1.5–2 times larger than that of neat matrix polymer. The tensile strengths of the nanocomposites were almost the same as that of the neat matrix polymer. However, the Young's modulus of our nanocomposites was about 11% larger than that of neat PS. Therefore, we need a new contraption to get nanocomposites with fully exfoliated clay platelets. In future works, we will investigate the optimized compounding ratio of OPS, develop a new organic modifier of clay for a nanocomposite with fully exfoliated clay platelets by melt compounding, and develop a screw design for the good melt compounding of PS/clay systems.

The authors would like to thank the Plastic Technical Center, Sumitomo Chemicals Co., Ltd., Japan, for taking TEM photographs.

References

1. Utracki, L. A. Clay-Containing Polymeric Nanocomposites; RAPRA Technology: Shrewsbury, Shropshire, UK, 2004.
2. Okada, A.; Usuki, A. *Mater Sci Eng C* 1995, 3, 109.
3. Dennis, H. R.; Hunter, D. L.; Chang, D.; Kim, S.; White, J. L.; Cho, J. W.; Paul, D. R. *Polymer* 2001, 42, 9513.
4. Davis, C. H.; Mathias, L. J.; Gilman, J. W.; Schiraldi, D. A.; Shields, J. R.; Trulove, P.; Sutto, T. E.; Hugh, G. D. *J Polym Sci Part B: Polym Phys* 2002, 40, 2661.
5. Shah, R. K.; Paul, D. R. *Polymer* 2004, 45, 2991.
6. Fornes, T. D.; Yoon, P. J.; Keskkula, H.; Paul, D. R. *Polymer* 2001, 42, 9929.
7. Hasegawa, N.; Okamoto, H.; Kato, M.; Usuki, A.; Sato, N. *Polymer* 2003, 44, 2933.
8. Yoon, P. J.; Hunter, D. L.; Paul, D. R. *Polymer* 2003, 44, 5323.
9. Yoon, P. J.; Hunter, D. L.; Paul, D. R. *Polymer* 2003, 44, 5341.
10. Wang, Y.; Chen, F.-B.; Wu, K.-C. *J Appl Polym Sci* 2004, 93, 100.
11. Arazi, N.; Nir, Y.; Narkis, M.; Siegmann, A. *J Polym Sci Part B: Polym Phys* 2002, 40, 1741.
12. Gianelli, W.; Camino, G.; Dintcheva, N. T.; Lo Verso, S.; La Manita, F. P. *Macromol Mater Eng* 2004, 289, 238.
13. Yasmin, A.; Abot, J. L.; Daniel, I. M. *Scr Mater* 2003, 49, 81.
14. Pluta, M.; Galeski, A.; Alexandre, M.; Paul, M.-A.; Dubois, P. *J Appl Polym Sci* 2002, 86, 1497.
15. Tanoue, S.; Utracki, L. A.; Garcia-Rejon, A.; Tatibouët, J.; Cole, K. C.; Kamal, M. R. *Polym Eng Sci* 2004, 44, 1046.
16. Tanoue, S.; Utracki, L. A.; Garcia-Rejon, A.; Sammut, P.; Ton-That, M.-T.; Peaneau, I.; Kamal, M. R.; Lyngaae-Jørgensen, J. *Polym Eng Sci* 2004, 44, 1061.
17. Tanoue, S.; Utracki, L. A.; Garcia-Rejon, A.; Tatibouët, J.; Kamal, M. R. *Polym Eng Sci* 2005, 45, 827.
18. Wang, H.; Zeng, C.; Elkovitch, M.; Lee, L. J.; Koelling, K. W. *Polym Eng Sci* 2001, 41, 2036.
19. Hoffmann, B.; Dietrich, C.; Thomann, R.; Friedrich, C.; Mulhaupt, R. *Macromol Rapid Commun* 2000, 21, 57.
20. Hasegawa, N.; Kawasumi, M.; Kato, M.; Usuki, A.; Okada, A. *J Appl Polym Sci* 1998, 67, 87.
21. Hasegawa, N.; Okamoto, H.; Kawasumi, M.; Usuki, A. *J Appl Polym Sci* 1999, 74, 3359.
22. Yoon, J. T.; Jo, W. H.; Lee, M. S.; Ko, M. B. *Polymer* 2001, 42, 329.